ARTICLE

Gold Nanoparticle-Based Miniaturized Nanomaterial Surface Energy Transfer Probe for Rapid and Ultrasensitive Detection of Mercury in Soil, Water, and Fish

Gopala Krishna Darbha, Anandhi Ray, and Paresh Chandra Ray*

Department of Chemistry, Jackson State University, Jackson, Mississippi 39217

ABSTRACT Contamination of the environment with mercury has been an important concern throughout the world for decades. Exposure to high Hg levels can be harmful to the brain, heart, kidneys, lungs, and immune system of humans of all ages. Driven by the need to detect trace amounts of mercury in environmental samples, here we present a miniaturized, inexpensive, and battery-operated ultrasensitive gold nanoparticle-based nanomaterial surface energy transfer probe for screening mercury levels in contaminated soil, water, and fish which has excellent sensitivity (2 ppt) and selectivity for Hg(II) over competing analytes, with the largest fluorescence enhancement to date for sensing Hg(II) in environmental samples (1100-fold). The sensitivity of our probe to detect mercury level in soil, water, and fish is about 2–3 orders of magnitude higher than the EPA standard limit. We demonstrate that our probe is suitable to screen the amount of mercury in different fish, shellfish, and water samples from various commercial sources.

KEYWORDS: NSET · nanoprobe · gold nanoparticle · mercury detection · environmental samples

Mercury is a known environmental pollutant routinely released from coal-burning power plants, oceanic and volcanic emissions, gold mining, and solid waste incineration.[1] The long atmospheric residence time of Hg^0 vapor and its oxidation to soluble inorganic Hg(II) provide a pathway for contaminating vast amounts of water and soil. Bacteria living in the sediments of aqueous environments transform inorganic Hg(II) into methylmercury, a potent neurotoxin that concentrates through the food chain in the tissues of fish and marine mammals. Subsequent ingestion of methylmercury by humans from seafood and other dietary and environmental sources is connected to serious sensory, motor, and cognitive disorders. Since exposure to high Hg levels can be harmful to the brain, heart, kidneys, lungs, and immune system of humans of all ages, it is important to develop an extremely high-sensitivity, cost-effective Hg sensor that can provide real-time determination of Hg levels in the environment, water, and food. Several methods,[2–5] such as atomic absorption and fluorescence spectroscopy, inductively coupled plasma atomic emission spectrometry, electrochemical sensoring, and the use of piezoelectric quartz crystals, provide limits of detection at the parts-per-billion (ppb) level. Although these approaches provide low detection limits, these methods are time-consuming and laborious, and they lack the procedural simplicity for on-site analysis. To avoid this, alternative approaches using fluorescence-based molecular sensors and chemosensors[5–10] have been actively pursued. However, most of these sensors display drawbacks in terms of actual applicability, such as the lack of water solubility, cross-sensitivity toward other metal ions, weak fluorescence enhancement factors, and short emission wavelengths.

There have been many recent efforts toward the development of fluorescence assays for mercury detection, based on fluorescence resolance energy transfer (FRET) or non-FRET quenching mechanisms. FRET is a spectroscopic technique in which excitation energy of the donor is transferred to the acceptor *via* an induced-dipole–induced-dipole interaction. Although FRET technology is very convenient and can be applied routinely at the single-molecule detection limit, the efficiency of FRET is very sensitive to the distance between the donor and an acceptor. The length scale for detection using FRET-based methods is limited by the nature of the dipole–dipole

*Address correspondence to paresh.c.ray@jsums.edu.

Received for review May 2, 2007 and accepted September 28, 2007.

Published online October 31, 2007. 10.1021/nn7001954 CCC: $37.00

mechanism, which effectively constrains the length scales to distances on the order of <100 Å ($R_0 \approx 60$ Å). The limitations of FRET can be overcome with a dynamic molecular ruler based on the distance-dependent plasmon coupling of metal nanoparticles.[22–30] Recently, several groups, including ours,[22–30] have reported that nanomaterial surface energy transfer (NSET) is a technique capable of measuring distances nearly twice as far as FRET in which energy transfer from a donor molecule to a nanoparticle surface follows a predictable distance dependence. In this article, we present a gold nanoparticle-based miniaturized, inexpensive, and battery-operated ultrasensitive NSET probe for screening mercury levels in water and fish, which has excellent sensitivity (2 ppt) and selectivity for Hg(II) over competing analytes, including common metal ion contaminants such as Cu^{2+} and Pb^{2+}, with the largest fluorescence enhancement to date for sensing Hg(II) in water (1100-fold). A battery-operated laser pointer induced the fluorescence from rhodamine B. The compact architecture of the designed sensor, along with the carefully aligned optics, offers a cost-effective way to detect mercury in water with a detection limit at the parts-per-trillion (ppt) level. Experiments with contaminated soils and fish collected from the field show that our nanoparticle probe is capable of reliably detecting mercury levels in environmental samples at the parts-per-trillion level.

RESULTS AND DISCUSSIONS

Our mercury detection approach is based on the use of gold nanoparticle-based NSET[11–20] (where the gold nanoparticle surface acts as an acceptor and organic dye acts as a donor) which provides high sensitivity for the detection of metal ions because of their unique property of superquenching chromophores through both energy-transfer and electron-transfer processes. Rhodamine B molecules, which are highly fluorescent (fluorescence quantum yield 0.70) in aqueous solution, were self-adsorbed onto the surface of gold nanoparticles (see Figure 1).

Our experimental data showed a quenching efficiency of nearly 100% when the fluorophore was statically adsorbed on the particle (static quenching). The fluorophore is completely quenched by efficient nonradiative energy transfer to the gold particle, and the strong quenching abilities of colloidal gold are related to its large molar extinction coefficients ($\sim 10^{10}$ cm^{-1} M^{-1} for 20–30 nm particles) and its nanomolar binding affinities for organic dyes. Like normal FRET, the interaction for gold nanomaterial-based surface energy transfer is dipole–dipole in nature but is geometrically different because the acceptor nanoparticle has a surface and an isotropic distribution of dipole vectors to accept energy from the donor. This arrangement increases the probability of energy transfer and accounts

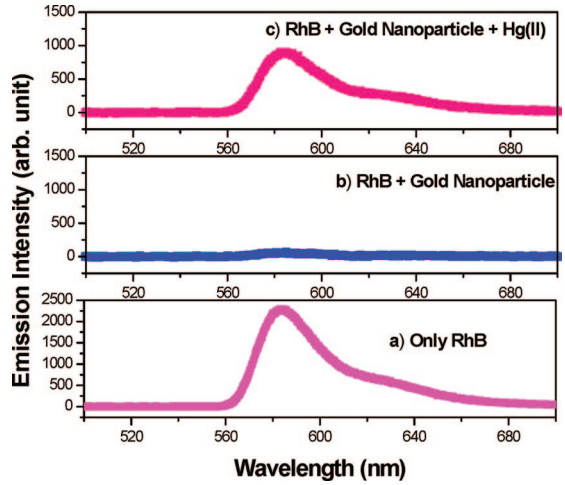

Figure 1. Plot of fluorescence intensity *vs* wavelength: (a) rhodamine B (RhB) dye in water solution (5.6 μM); (b) RhB self-adsorbed onto gold nanoparticles in 5 nM solution; (c) 130 ppb Hg(II) added to solution (b) (RhB-adsorbed gold nanoparticle solution).

for the enhanced efficiency for gold nanomaterial-based NSET over normal FRET.

In the presence Hg(II) ions, rhodamine B molecules are released from the gold nanoparticle surface, and thus we observed a very distinct fluorescence signal change (Figure 1b). Fluorescence signal enhancement by a factor of 800 was observed within a few seconds after the addition of 130 ppb of mercury (Figure 1c). Since the energies for surface adsorption of organic dyes onto gold are usually in the range of 8–16 kcal/mol, much smaller than the binding energies involved in rhodamine B and mercury binding (80–100 kcal/mol), after addition of Hg(II) the fluorophore is separated from the nanoparticle surface, resulting in an 800-fold increase in fluorescence signal.

To determine whether the changes of the rhodamine B fluorescence observed on the gold nanoparticle surface are due mainly to NSET, we performed the same experiment on a gold nanorod surface (see Supporting Information for synthesis and characterization of gold nanorod), as shown in Figure 2. Since gold nanorods of 80 nm length and 22 nm width show a strong longitudinal plasmon band at 700 nm and a very weak transverse plasmon band at 510 nm (as shown in the Supporting Information), we expect very little quenching to occur when RhB is adsorbed onto the gold nanorod surface. Our results indicate only 7–10% quenching (Figure 2b). We did not observe any real change of the fluorescence signal after addition of 130 ppb of mercury (Figure 2c), whereas we observed fluorescence signal enhancement by a factor of 800 within a few seconds after the addition of 130 ppb of mercury onto the gold nanoparticle surface, which exhibits a very strong absorption band around 550 nm ($\epsilon \approx 10^{10}$ cm^{-1} M^{-1}). This indicates that the observed changes of rhodamine B fluorescence on the gold nanoparticle surface are due mainly to NSET. Since we have not ob-

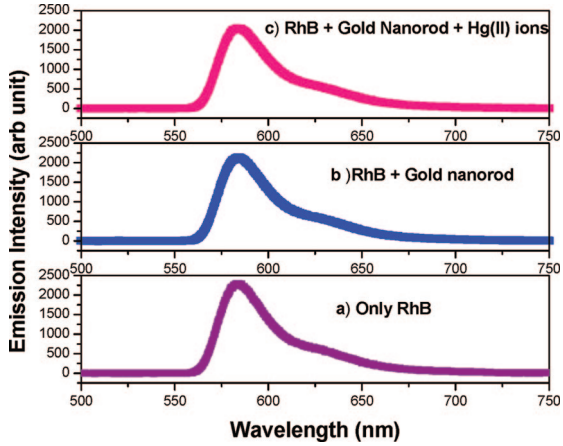

Figure 2. Plot of fluorescence intensity *vs* wavelength: (a) rhodamine B (RhB) dye in water solution (5.6 μM); (b) RhB self-adsorbed on gold nanorods in 5 nM solution; (c) 130 ppb Hg(II) added to solution (b) (RhB-adsorbed gold nanorod solution).

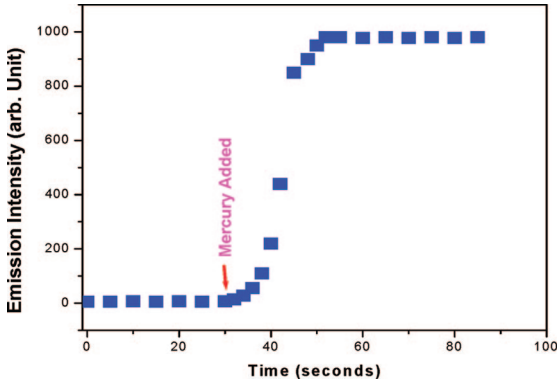

Figure 3. Plot of fluorescence intensity *vs* time (in seconds) upon the addition of 130 ppb Hg(II) to RhB-adsorbed gold nanoparticle solution. The arrow indicates the initial time of mercury addition.

served any significant shift of fluorescence maximum wavelength for RhB after addition of mercury, either to gold nanorod surface (Figure 2) or to gold nanoparticle surface (as shown in Figure 1), we believe that there is no bond dissociation, oxidation, or reduction reaction of RhB in the presence of mercury. We also have not observed any significant shift of the absorption maximum of RhB or appearance of a new peak in the absorption spectra due to the addition of mercury to RhB solution.

To understand the response rate of the fluorescence signal upon addition of Hg(II), we have measured the fluorescence intensity at different time intervals, as shown in Figure 3, where the arrow indicates the initial time of Hg(II) addition. Our experimental data indicate that, after addition of 130 ppb of Hg(II), the fluorescence intensity increases by a factor of 800 within 20 s and then remains constant with time, which indicates that the reaction is complete. Our time interval of fluorescence intensity measurement indicates that the time frame of our measurement is only 20 s.

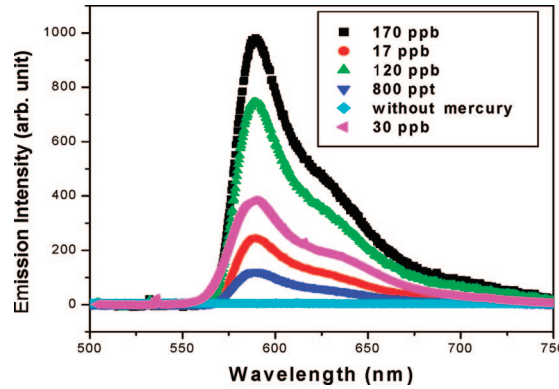

Figure 4. Fluorescence response of RhB adsorbed onto gold nanoparticles in 5 nM solution upon addition of different concentrations of Hg(II) ions (800 ppt, 17 ppb, 30 ppb, 120 ppb, and 170 ppb).

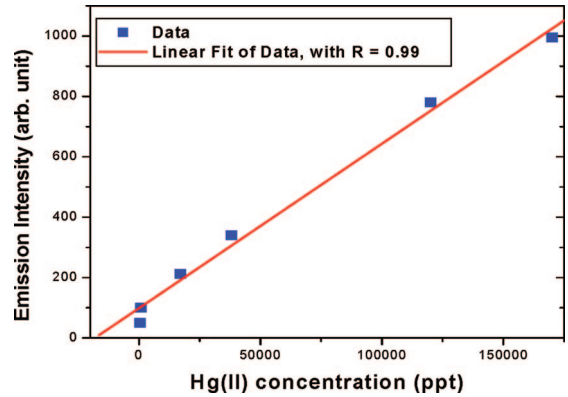

Figure 5. Plot of fluorescence intensity *vs* Hg(II) concentration in parts-per-trillion. A linear correlation exists over the range of 0.8–170 ppb, with $R = 0.99$.

To evaluate the sensitivity of our NSET probe, different concentrations of Hg(II) from one stock solution were evaluated. As shown in Figure 4, the NSET emission intensity is highly sensitive to the concentration of Hg(II) ions, and the intensity increased linearly with concentration of Hg(II) ions. A linear correlation was found between the emission intensity and concentration of Hg(II) ions over the range of 0.8–170 ppb, as shown in Figure 5. The U.S. Environmental Protection Agency (EPA) standard for the maximum allowable level of Hg(II) in drinking water is 2 ppb. Our experiment indicates that our gold nanoparticle-based FRET probe is capable of measuring Hg(II) concentration even at the 2 ppt level, which is 4 orders of magnitude lower than the EPA standard, and it provides a sensitivity which is about an order of magnitude higher than the previously reported data using any established technique or fluorescence-based or gold nanoparticle-based technique[21–26] for sensing heavy metals.

For fluorescence excitation, we have used a CW Melles-Griot green laser pointer (18 Lab 181), operating at 532 nm, as an excitation light source. The laser pointer can be operated for 10–13 h with two AAA size batteries, and its maximum output power is ~5 mW. This light source has a capability to minimize the whole

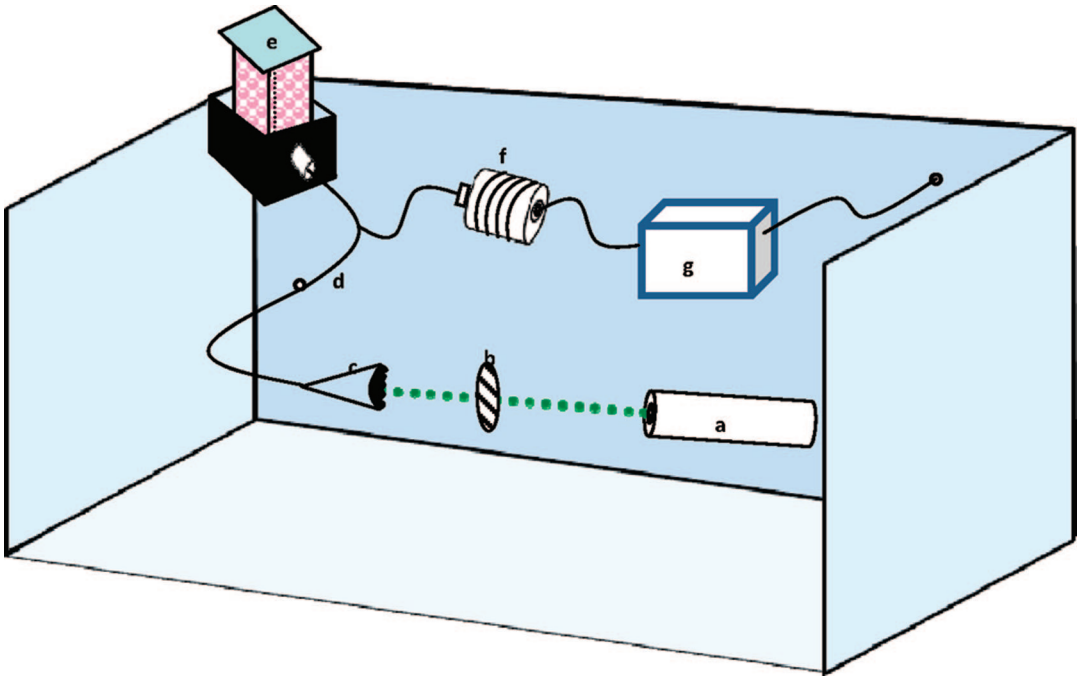

Scheme 1. Schematic diagram of our NSET probe. It consists of several components: (a) Melles-Griot green laser pointer (18 Lab 181), (b) neutral density filter, (c) plano-convex lens, (d) optical fiber, (e) sample holder, (f) 532 nm cut-off filter, and (g) Ocean Optics QE65000 spectrometer.

sensor configuration. In this minimized configuration (see Scheme 1), we have incorporated an Ocean Optics CUV-ALL-UV four-way cuvette holder equipped with fiber-optic couplings at each of four quartz *f*/2 collimating lenses, which couple to optical fibers to either read or illuminate the sample. We have used a 200 μm illumination fiber and a 50 μm read fiber. The collected laser-induced fluorescence (LIF) signal was fed into a highly sensitive Ocean Optics QE65000 spectrometer (90% quantum efficiency with high signal-to-noise and rapid signal processing speed). The LIF spectrum was collected with Ocean Optics data acquisition software. All measurements were performed with 5 ms integration time and were instantaneously averaged for five spectra using the software. The averaged data were processed using a Microsoft Excel program. The total size of the sensor system was 6 in. × 12 in. × 6 in., including the laser pointer, optical fibers, and spectrometer in an aluminum box (Scheme 1). The ON/OFF (push/pull) switch of the laser pointer is located at the other end of the laser pointer and is fixed in such a way that one can operate it from outside of the aluminum box.

To detect Hg(II) ions selectively, we modified the surface of the gold nanoparticle with mercaptopropionic acid (MPA) and homocystine (bound to the gold nanoparticle surface through a Au–S bond), and we added a chelating ligand, 2,6-pyridinedicarboxylic acid (PDCA), to the solution. It has been reported[27] in the literature that the stability constants between heavy metal ions and chelating ligands like MPA are log K(Pb) = 4.1, log K(Hg) = 10.1, log K(Cd) = 3.2, and log K(Zn) = 1.8. Therefore, the stability constant of the mercury–MPA complex is about 6 orders of magnitude higher than those of other interfering metal ions. Figure 6 shows the

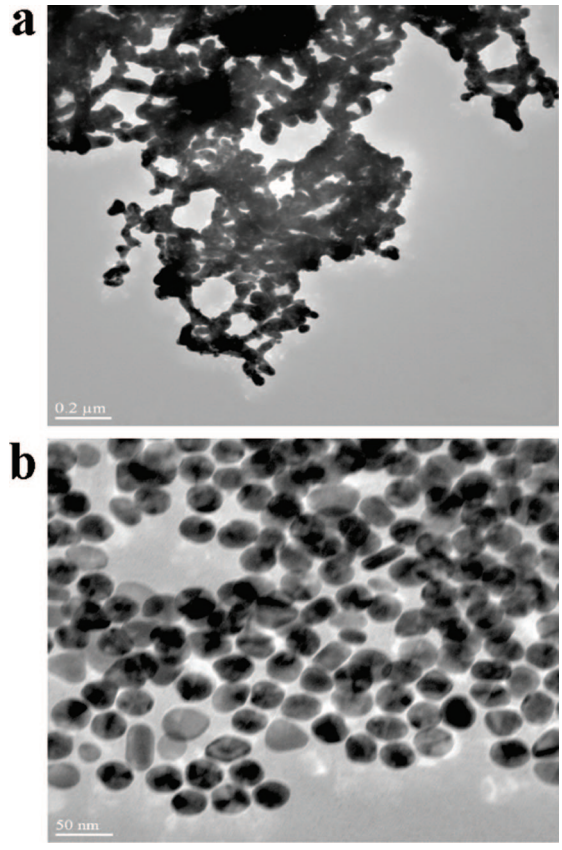

Figure 6. TEM images of a gold nanoparticle–MPA solution (a) in the presence and (b) in the absence of 130 ppm Hg(II) ions.

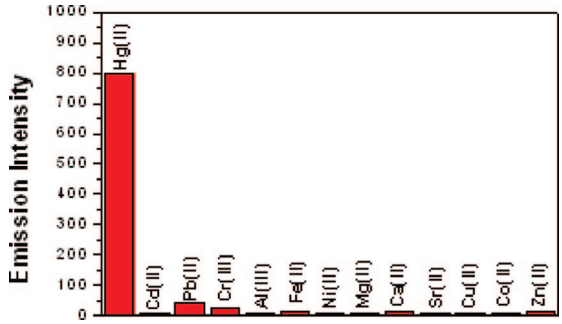

Figure 7. Fluorescence response upon the addition of 130 ppb of different metal ions on RhB-adsorbed gold nanoparticle–MPA–PDCA solution (5 nM).

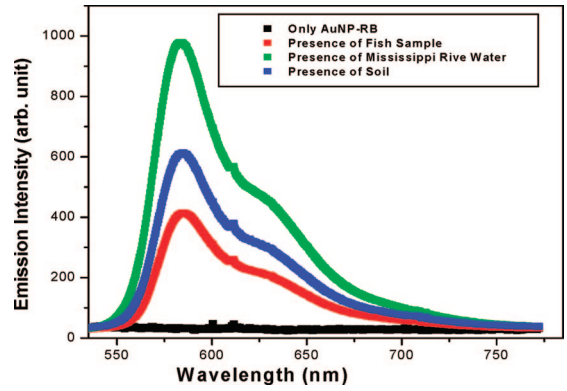

Figure 8. Fluorescence response of RhB-adsorbed 5 nM gold nanoparticle–MPA–PDCA solution in the absence and in the presence of different environmental samples (fish, water, and soil) of the same amount.

TEM images of a gold nanoparticle–MPA solution in the presence and in the absence of Hg(II) ions. Due to strong binding of Hg(II) with chelating ligands like MPA, aggregation of gold nanoparticles in the presence of Hg(II) ions was observed in our TEM image (Figure 6a). Our results indicate that, just by modifying the gold nanoparticle surface with MPA, our sensor has 6–10 times higher sensitivity toward mercury ions than that toward Cd, Pb, and Zn ions.

Further higher selectivity of our probe toward Hg(II) ions was achieved by adding a chelating ligand, PDCA. Stability constants of heavy metal ions with PDCA are log K(Pb) = 8.2, log K(Hg) = 20.2, log K(Cd) = 10.0, and log K(Mn) = 8.5.[28] Therefore, PDCA will be able to form a much more stable complex with Hg(II) than with other metal ions. To achieve better selectivity, we added PDCA to each MPA–gold nanoparticle solution at a concentration about 7–10 times greater than that of Hg(II) ions. We noted the shift in the plasmon band energy to longer wavelength (about 150–200 nm) after the addition of Hg(II) ions to the MAP–gold nanoparticle–PDCA solution, which indicated strong aggregation of gold nanoparticles due to Hg(II) binding with chelating ligands, yielding both a substantial shift in the plasmon band energy to longer wavelength and a red-to-blue color change. Our results indicate that, upon modifying the gold nanoparticles with both MPA and PDCA, selectivity toward mercury ions increases 40–60 times compared to that toward Cd, Pb, and Zn ions. Figure 7 shows the fluorescence response of our NSET probe in the presence of various environmentally relevant metal ions. Our result shows excellent selectivity (as shown in Figure 7) for Hg(II) over alkali, alkaline earth (Li^+, Na^+, K^+, Mg^{2+}, Ca^{2+}), and transition heavy metal ions (Pb^{2+}, Pb^+, Mn^{2+}, Fe^{2+}, Cu^{2+}, Ni^{2+}, Zn^{2+}, Cd^{2+}). We believe that PDCA ligands bound to the MPA–AuNP species through Au–N bonds improve the selectivity toward Hg(II) ions through a cooperative effect, while the PDCA ligands in the bulk solutions form complexes with the other metal ions, suppressing their interference with the probes.

To evaluate whether our NSET probe can detect Hg(II) ions from environmental samples, we have measured mercury content in water, soils, and fish collected from the Mississippi River. Fish collected from the river were dissolved in HNO_3, and the resulting solutions were brought to pH 7. Soil from the Mississippi River was dissolved in Aqua Regia, and then microwave treatments were performed as reported in the literature,[29] and the resulting solutions were brought to pH 7. Mercury content was measured using our nanoparticle-based NSET probe (as shown in Figure 8) and also verified using inductively coupled plasma mass spectrometry (ICPMS). The amount of Hg(II) measured in soil samples by our method was in very good agreement (90–95%) with ICPMS values.

Once we confirmed that our nanoparticle-based NSET probe is able to detect Hg(II) ions selectively from environmental samples, the probe was applied to provide a rapid screening for total mercury content in water and fish from different sources. Mercury content was verified by our nanoparticle-based NSET method as well as by the ICPMS technique. Figure 9 shows the NSET response from different water samples collected from the Mississippi River, Lakeland Lake, tap water, and drinking water. Our NSET data indicate that the mercury level in the Mississippi River is quite high and the level of mercury in drinking and tap water samples is

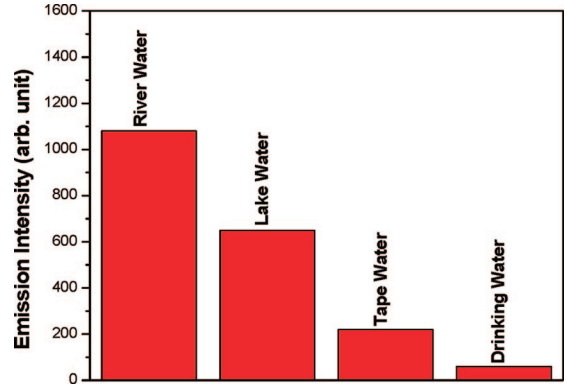

Figure 9. Fluorescence response of RhB-adsorbed 5 nM gold nanoparticle–MPA–PDCA solution upon the addition of water samples (300 μL) from different sources.

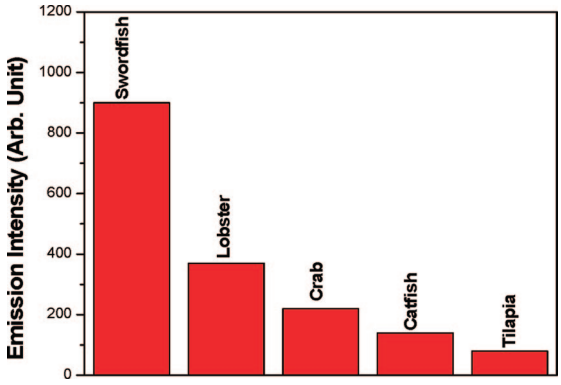

Figure 10. Fluorescence response of RhB-adsorbed 5 nM gold nanoparticle–MPA–PDCA solution upon the addition of different fish samples in the same amounts (100 μg).

much less than the EPA limit of 2 ppb. ICPMS data for Mississippi River water and Lakeland lake water match our NSET data to within 95%.

To determine the concentration of Hg(II) in fish samples, we used a standard addition method. We observed a good linear emission response, and the total mercury content was 0.1–0.005 ppm, which indicates that our NSET probe is capable of distinguishing safe and toxic levels of mercury in fish samples according to the 0.55 ppm U.S. EPA standard. The Hg(II) content measured in fish samples by our method was in very good agreement (92–98%) with ICPMS values. Figure 10 shows the fluorescence response of our NSET probe from samples of different fish. Our NSET probe data indicate that swordfish contain mercury at levels a little higher than the EPA limit of 0.55 ppm, whereas the amounts of mercury in other fish and shellfish, *e.g.*, lobster, crab, catfish, and tilapia, are lower than the EPA limit. Our data match within 85–92% the reported data available in the literature.[30]

CONCLUSION

In conclusion, in this article we have reported a miniaturized, inexpensive, and battery-operated ultrasensitive gold nanoparticle-based NSET probe for screening mercury levels in soil, fish, and water with excellent sensitivity (2 ppt) and selectivity for Hg(II) over competing analytes. Our probe exhibits the largest fluorescence enhancement to date for sensing Hg(II) in water. Furthermore, the sensitivity of our probe to detect mercury levels in soil, water, and fish is about 2–3 orders of magnitude higher than the EPA standard limit. We have shown that our probe is suitable to screen the amount of mercury in different fish, shellfish, and water samples from various commercial sources. Though we have demonstrated this only for soil, water, and fish samples, we believe that our probe provides a useful starting point for the development of a practical nanosensor for screening mercury from a wide range of biological, toxicological, and environmental samples.

MATERIALS AND EXPERIMENTS

Hydrogen tetrachloroaurate ($HAuCl_4 \cdot 3H_2O$), $NaBH_4$, rhodamine B dye, mercaptopropionic acid (MPA), homocystine (HCys), 2,6-pyridinedicarboxylic acid, buffer solution, sodium chloride, and sodium citrate were purchased from Sigma-Aldrich and used with out further purification.

Gold Nanoparticle Synthesis. Gold nanoparticles of 15 nm or larger diameters were synthesized using reported methods.[11–13] Gold nanoparticles of different sizes and shapes were synthesized by controlling the ratio of $HAuCl_4 \cdot 3H_2O$ and sodium citrate concentration as we reported recently.[11–13] For smaller gold nanoparticles, we used a sodium borohydride method as reported previously. A 0.5 mL amount of 0.01 M $HAuCl_4 \cdot 3H_2O$ in water and 0.5 mL of 0.01 M sodium citrate in water were added to 18 mL of deionized H_2O and stirred. Next, 0.5 mL of freshly prepared 0.1 M $NaBH_4$ was added, and the solution changed from colorless to orange. Stirring was stopped, and the solution was left undisturbed for 2 h. The resulting spherical gold nanoparticles were 4 nm in diameter. Transmission electron microscopy (TEM) and UV–visible absorption spectroscopy were used to characterize the nanoparticles. The particle concentration was measured by UV–visible spectroscopy using the molar extinction coefficients at the wavelength of the maximum absorption of each gold colloid, as reported recently[11] [$\epsilon_{(15)528nm} = 3.6 \times 10^8\ cm^{-1}\ M^{-1}$, $\epsilon_{(30)530nm} = 3.0 \times 10^9\ cm^{-1}\ M^{-1}$, $\epsilon_{(40)533nm} = 6.7 \times 10^9\ cm^{-1}\ M^{-1}$, $\epsilon_{(50)535nm} = 1.5 \times 10^{10}\ cm^{-1}\ M^{-1}$, $\epsilon_{(60)540nm} = 2.9 \times 10^{10}\ cm^{-1}\ M^{-1}$, and $\epsilon_{(80)550nm} = 6.9 \times 10^{10}\ cm^{-1}\ M^{-1}$].

Gold Nanoparticle Surface Modification. MPA and HCys were attached to the gold nanoparticle surface through –SH bonds using a method similar to one we have described before. We added 10 mM MPA (10 μL) and 10 mM HCys (10 μL) to the gold nanoparticle solution (15 nM, 10 mL) with stirring. After 2 h, 5–8 mM $NaBH_4$ was added. Finally, 1 mL of 5×10^{-4} M aqueous rhodamine B solution was added to 9 mL of the 15 nM gold nanoparticle solution, and the mixture was left for a few hours without disturbance.

Fish Assay. We have used a method similar to the one described before.[10] OmniTrace Ultra-grade nitric acid (EM Science) was used for digestion experiments. All glassware was rinsed with dilute nitric acid and Millipore water before use. Samples of fish tissue (0.2 g) were dissected from frozen whole specimens after scale removal and digested in nitric acid (5 mL) at 180 °C for 5–10 min. The resulting solutions were neutralized with NaOH and HEPES to pH 7.

Acknowledgment. P.C.R. thanks NSF-PREM grant no. DMR-0611539, NSF-CRIFMU grant no. 0443547, and NSF-MRI grant no. 0421406 for generous funding. We thank Sara H. Bayley, Instrumentation Facilities Coordinator, University of Southern Mississippi, for helping to acquire TEM data. We also thank reviewers whose valuable suggestions improved the quality of the manuscript.

Supporting Information Available: Synthesis and characterization of gold nanorods. This material is available free of charge *via* the Internet at http://pubs.acs.org.

REFERENCES AND NOTES

1. U.S. EPA. Regulatory Impact Analysis of the Clean Air Mercury; EPA-452/R-05-003; U.S. Government Printing Office: Washington, DC, 2005.
2. Butler, O. T.; Cook, J. M.; Harrington, C. F.; Hill, S. J.; Rieuwerts, J.; Miles, D. L. J. Atomic Spectrometry Update. Environmental Analysis. *Anal. At. Spectrom.* **2006**, *21*, 217–243.
3. Li, Y.; Chen, C.; Li, B.; Sun, J.; Wang, J.; Gao, Y.; Zhao, Y.; Chai, Z. J. Elimination Efficiency of Different Reagents for

the Memory Effect of Mercury Using ICP-MS. *Anal. At. Spectrom.* **2006**, *21*, 94–96.
4. Leermakers, M.; Baeyens, W.; Quevauviller, P.; Horvat, M. Mercury in Environmental Samples: Speciation, Artifacts and Validation. *Trends Anal. Chem.* **2005**, *24*, 383–393.
5. *Molecular Fluorescence: Principles and Applications*; Valeur, B., Ed.; Wiley-VCH: Weinheim, 2002.
6. Komatsu, H.; Miki, T.; Citterio, D.; Kubota, T.; Shindo, Y.; Kitamura, Y.; Oka, K.; Suzuki, K. Single Molecular Multianalyte (Ca^{2+}, Mg^{2+}) Fluorescent Probe and Applications to Bioimaging. *J. Am. Chem. Soc.* **2005**, *127*, 10798–10799.
7. Zhu, X.-J.; Fu, S.-T.; Wong, W.-K.; Guo, J.-P.; Wong, W.-Y. A Near-Infrared-Fluorescent Chemodosimeter for Mercuric Ion Based on an Expanded Porphyrin. *Angew. Chem., Int. Ed.* **2005**, *45*, 3150–3154.
8. Mello, J. V.; Finney, N. S. Reversing the Discovery Paradigm: A New Approach to the Combinatorial Discovery of Fluorescent Chemosensors. *J. Am. Chem. Soc.* **2005**, *127*, 10124–10125.
9. Nolan, E. M.; Lippard, S. J. A "Turn-On" Fluorescent Sensor for the Selective Detection of Mercuric Ion in Aqueous Media. *J. Am. Chem. Soc.* **2003**, *125*, 14270–14271.
10. Caballero, A.; Martínez, R.; Lioveras, V.; Tatera, I.; Vidal-Gancedo, J.; Wurst, K.; Tárraga, A.; Molina, P.; Veciana, J. Highly Selective Chromogenic and Redox or Fluorescent Sensors of Hg^{2+} in Aqueous Environment Based on 1,4-Disubstituted Azines. *J. Am. Chem. Soc.* **2005**, *127*, 15666–15667.
11. Ray, P. C.; Fortner, A.; Darbha, G. K. Gold Nanoparticle Based FRET Asssay for the Detection of DNA Cleavage. *J. Phys. Chem. B* **2006**, *110*, 20745–20748.
12. Ray, P. C. Label-Free Diagnostics of Single Base-Mismatch DNA Hybridization on Gold Nano-Particles Using Hyper-Rayleigh Scattering Technique. *Angew. Chem.* **2006**, *45*, 1151–1154.
13. Kim, C. K.; Kalluru, R. R.; Singh, J. P.; Fortner, A.; Griffin, J.; Darbha, G. K.; Ray, P. C. Gold Nanoparticle Based Miniaturized Laser Induced Fluorescence Probe for Specific DNA Hybridization Detection: Studies on Size Dependent Optical Properties. *Nanotechnology* **2006**, *17*, 3085.
14. Jennings, T. L.; Singh, M. P.; Strouse, G. F. Fluorescent Lifetime Quenching near $d = 1.5$ nm Gold Nanoparticles: Probing NSET Validity. *J. Am. Chem. Soc.* **2006**, *128*, 5462.
15. Dubertret, B.; Calame, M.; Libchaber, A. J. Single-Mismatch Detection Using Gold-Quenched Fluorescent Oligonucleotides. *Nat. Biotechnol.* **2001**, *19*, 365–370.
16. Thaxton, C. S.; Mirkin, C. A. Plasmon Coupling Measures Up. *Nature Biotechnol.* **2005**, *23*, 681–682.
17. Sonnichsen, C.; Reinhard, B. M.; Liphardt, J.; Alivisatos, A. P. A Molecular Ruler Based on Plasmon Coupling of Single Gold and Silver Nanoparticles. *Nature Biotechnol.* **2005**, *23*, 741–745.
18. Famulok, M.; Mayer, G. Aptamers in Nanoland. *Nature* **2006**, *439*, 666–669.
19. Maxwell, D. J.; Taylor, J. R.; Nie, S. Self-Assembled Nanoparticle Probes for Recognition and Detection of Biomolecules. *J. Am. Chem. Soc.* **2002**, *124*, 9602.
20. Fan, C.; Wang, S.; Hong, J. W.; Bazan, G. C.; Plaxco, K. W.; Heeger, A. J. Beyond Superquenching: Hyper-Efficient Energy Transfer from Conjugated Polymers to Gold Nanoparticles. *Proc. Natl. Acad. Sci. U.S.A.* **2003**, *100*, 6297–6301.
21. Rex, M.; Hernandez, F. E.; Campiglia, A. D. Pushing the Limits of Mercury Sensors with Gold Nanorods. *Anal. Chem.* **2006**, *78*, 445–451.
22. Kim, Y.; Johnson, R. C.; Hupp, J. T. Gold Nanoparticle-Based Sensing of "Spectroscopically Silent" Heavy Metal Ions. *Nano Lett.* **2001**, *1*, 165–167.
23. Liu, J.; Lu, Y. Stimuli-Responsive Disassembly of Nanoparticle Aggregates for Light-Up Colorimetric Sensing. *J. Am. Chem. Soc.* **2005**, *127*, 12677–12683.
24. Huang, C.-C.; Chang, H.-T. Selective Gold-Nanoparticle-Based "Turn-On" Fluorescent Sensors for Detection of Mercury(II) in Aqueous Solution. *Anal. Chem.* **2006**, *78*, 8332–8338.
25. Wanunu, M.; Popovitz-Biro, R.; Cohen, H.; Vaskevich, A.; Rubinstein, I. Coordination-Based Gold Nanoparticle Layers. *J. Am. Chem. Soc.* **2005**, *127*, 9207–9215.
26. He, X.; Liu, H.; Li, Y.; Wang, S.; Li, Y.; Wang, N.; Xiao, J.; Xu, X.; Zhu, D. Gold Nanoparticle-Based Fluorometric and Colorimetric Sensing of Copper(II) Ions. *Adv. Mater.* **2005**, *17*, 2811–2815.
27. Morel, F. M. M. *Principles of Aquatic Chemistry*; Wiley-Interscience: New York, 1983; 237–310.
28. Norkus, E; Stalnioniene, I.; Crans, D. C. Interaction of Pyridine- and 4-Hydroxypyridine-2,6-Dicarboxylic Acids with Heavy Metal Ions in Aqueous Solutions. *Heteroatom Chem.* **2003**, *14*, 625–632.
29. Bontidean, I; Mortari, A.; Leth, S. M.; Larsen, M. M.; Corbisher, P.; Csoregi, E. Biosensors for Detection of Mercury in Contaminated Soils. *Environ. Pollut.* **2004**, *131*, 255.
30. Mercury in fish: FDA monitoring, www.cfsan.fda.gov.